Mycelia Promote Active Transport and Spatial Dispersion of Polycyclic Aromatic Hydrocarbons

ARTICLE *in* ENVIRONMENTAL SCIENCE & TECHNOLOGY · MAY 2012

Impact Factor: 5.33 · DOI: 10.1021/es300810b · Source: PubMed

7 AUTHORS, INCLUDING:

Kevin C Jones
Lancaster University
668 PUBLICATIONS **29,272** CITATIONS
SEE PROFILE

Kirk T Semple
Lancaster University
185 PUBLICATIONS **5,958** CITATIONS
SEE PROFILE

Hauke Harms
Helmholtz-Zentrum für Umweltforschung
334 PUBLICATIONS **8,415** CITATIONS
SEE PROFILE

Lukas Y Wick
Helmholtz-Zentrum für Umweltforschung
127 PUBLICATIONS **2,911** CITATIONS
SEE PROFILE

Environmental Science & Technology

Article

pubs.acs.org/est

Mycelia Promote Active Transport and Spatial Dispersion of Polycyclic Aromatic Hydrocarbons

Shoko Furuno,[†] Susan Foss,[†] Ed Wild,[‡] Kevin C. Jones,[‡] Kirk T. Semple,[‡] Hauke Harms,[†] and Lukas Y. Wick*,[†]

[†]Department of Environmental Microbiology, Helmholtz Centre for Environmental Research - UFZ, Permoserstrasse 15, 04318 Leipzig, Germany

[‡]Lancaster Environment Centre, Lancaster University, Lancaster LA 1 4YQ, United Kingdom

Supporting Information

ABSTRACT: To cope with heterogeneous subsurface environments mycelial microorganisms have developed a unique ramified growth form. By extending hyphae, they can obtain nutrients from remote places and transport them even through air gaps and in small pore spaces, repectively. To date, studies have been focusing on the role that networks play in the distribution of nutrients. Here, we investigated the role of mycelia for the translocation of nonessential substances, using polycyclic aromatic hydrocarbons (PAHs) as model compounds. We show that the hyphae of the mycelial soil oomycete *Pythium ultimum* function as active translocation vectors for a wide range of PAHs. Visualization by two-photon excitation microscopy (TPEM) demonstrated the uptake and accumulation of phenanthrene (PHE) in lipid vesicles and its active transport by cytoplasmic streaming of the hyphae ('hyphal pipelines'). In mycelial networks, contaminants were translocated over larger distances than by diffusion. Given their transport capacity and ubiquity, hyphae may substantially distribute remote hydrophobic contaminants in soil, thereby improving their bioavailability to bacterial degradation. Hyphal contaminant dispersal may provide an untapped potential for future bioremediation approaches.

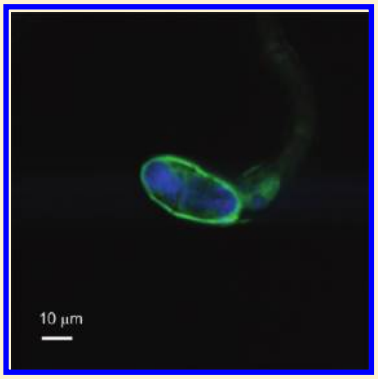

INTRODUCTION

To become effectively transformed by microorganisms, organic chemicals need to be transported at substantial mass fluxes to active degraders.[1] In the heterogeneous soil environment, this is often restricted by the propensity of many organic chemicals to accumulate in organic matter and micro- and nanopores; hence, escaping the aqueous microhabitats of the degrader organisms.[2] As a consequence, biotransformation of chemicals in soil is often limited by their low availability to degrading microorganisms.[3] Furthermore, contaminants may occur in microenvironments that are inhospitable to organisms as there is a lack of nutrients, water, or the appropriate electron acceptors. Mycelial organisms (e.g., filamentous fungi and oomycetes) exhibit a unique lifestyle to cope with such heterogeneous environments; the morphology of their mycelia reflects an effective foraging strategy combining highly explorative expansion under poor nutrient conditions with massive, exploitative growth in favorable environments.[4] Despite the microscopic nature of hyphae with diameters of 2−10 μm, fungi form some of the largest living organisms on Earth with reported networks extending over hundreds of hectares.[5] They represent about 75% of the subsurface microbial biomass (0.2−0.4 mg $g_{dry\ soil}^{-1}$) with networks of up to 10^3 to 10^4 m length per g of topsoil.[4] As a result, fungi and bacteria often occupy shared microhabitats.[6,7] By connecting air-filled space between water-filled pores,[8] fungi also provide efficient dispersal networks ('fungal highways'[9]) for random and targeted movement of otherwise immobilized bacteria. Experimental and simulation studies have also suggested that mycelia-mediated bacterial dispersal facilitates the access to suitable microhabitats for growth[10,11] and/or efficient contaminant biodegradation.[12−14] To maintain their extensive networks, mycelial microorganisms (independent of their physiological, functional and phylogenetical traits) have developed a highly polarized internal cellular organization that supports apical growth with interconnected vacuolar organelles thought to act as intracellular pathways for active and diffusive longitudinal transport[15,16] over distances of centimeters. The velocity of such cytoplasmic streaming typically ranges from 0.1−1.2 μm min^{-1} [17] to 600 μm min^{-1} [18] depending on the type of organism, its physiological state, or the location within the mycelium.

The observation of the fast active translocation of vacuoles in fungal mycelia made us speculate about the possibility that nonessential substances, such as hydrophobic organic compounds could be taken up by the hyphae and actively be translocated by their cytoplasmic streaming. A mycelium thus would function as a grid of 'pipelines' for contaminants.[19] Active contaminant translocation by the hyphal networks would occur at a higher rate than expected by diffusion alone. Uptake

Received: February 28, 2012
Revised: April 16, 2012
Accepted: April 19, 2012
Published: May 4, 2012

of contaminants by fungi has been reported for various chemicals including radionuclides,[20] heavy metals,[21] and organic pollutants.[22,23] Verdin et al.[22] showed that the uptake of PAH into a fungal mycelium is passive and that PAH are accumulated in lipid vesicles. Assuming however (i) reported PHE-lipid-water partitioning coefficients,[24] (ii) partitioning of hydrophobic compounds into the cytoplasmic triacylglycerol (TAG) storage lipids, and (iii) active lipid mobilization rates of 0.26−1.34 μg h^{-1} TAG per cross section area of main mycorrhizal runner hyphae,[25] initial calculations suggested that 10−50 pmol h^{-1} of PHE would be actively translocated by runner hyphae (as a rough proxy for other mycelial microorganisms). Here, we test the hypothesis that mycelia are effective vectors for the active transport of aromatic hydrocarbons by using the widespread soil oomycete *Pythium ultimum* as a model organism. Our data suggest that active transport of PAHs in mycelia may distribute contaminants further than passive mechanisms, such as diffusion.

MATERIAL AND METHODS

Organism, Culture Conditions, and Chemicals. Mycelial *P. ultimum*,[26] an easy to handle and fast growing pseudofungus that belongs to the stramenopiles group, was cultivated at room temperature (r.t.) on PDA (2%; Difco Laboratories, USA). 2,2,4,4,6,8,8-Heptamethylnonane (HMN; 98% purity; Aldrich, Germany) was used for dissolving a commercial PAH-mixture (PAH 63; Dr. Ehrenstorfer, Germany). PHE (≥97.0% HPLC), hexane (LiChrosolv grade), and acetone (99.8%) were obtained either from Fluka, Merck, or Roth (all Germany). PHE (99.9%) for two-photon excitation microscopy (TPEM) analysis was obtained from Aldrich (UK). Deuterated PAH surrogates and acenaphthylene (ACN-d_8) were used as recovery and injection standards (99.5%, Dr. Ehrenstorfer, Germany).

Experimental Test Tracks. *Column Test Track for the Quantification of PHE Transport.* A circular PDA piece (1 cm) freshly overgrown with *P. ultimum* was placed at the bottom of a sterile glass test tube (l: 12 cm; Ø: 1.0 cm) with a small hole (Ø: 0.1 cm) at its lower end for aeration (Figure S1). Solid PHE (20 mg) was sprinkled on the surface of *P. ultimum* and the mycelium first overlaid with a 1 cm thick layer of sterile, dry glass beads (Ø: 0.75−1 mm (Roth, Germany); porosity $\varphi \approx 0.4$) and second with a 0.5 cm thick layer of cleaned, dry Amberlite XAD4-resin (Sigma, Germany) to entrap PHE. A PDA patch was placed onto the resin to support growth of *P. ultimum* once it reached the top of the test track. The columns were loosely covered with sterile aluminum foil and incubated at r.t. in the dark. After 24, 48, 72, 96, 120, 168, 504, and 672 h the XAD4-entrapped PHE was quantified in triplicate experiments as detailed below. Mycelia-free experiments served as controls. The effective pore cross section of the column ($A_{ec} = \varphi \times A_c$) was calculated as 3.1×10^7 μm^2.

Calculations of Abiotic Transport of PHE in the Column Test Track. The abiotic PHE transport (F) was estimated by the diffusive PHE flux in pores[27] (eq 1)

$$F = -\theta_g \times D_e \times \delta C/\delta Z \quad (1)$$

θ_g is the volume of the gas-/water-filled pores of the medium, D_e is the effective PHE diffusion constant in air or water, δC is the maximal PHE vapor ($C_a = 7.2 \times 10^{-9}$ mol L^{-1}) or water ($C_w = 6.7 \times 10^{-6}$ mol L^{-1}) phase concentration gradient, and Z is the length (1 cm) of the glass bead layer. C_a at r.t. was calculated based on $C_i^\circ = P_i/RT$, where P is the PHE vapor pressure (0.063 atm at 25 °C[27]), R is the ideal gas constant (0.083 atm mol^{-1} K^{-1}), and T is the temperature (298 K). D_e relates to the diffusion constants D via $D_e = D/\tau_{uz}$ and $\tau_{uz} = \varphi^{5/2}/\theta_g$, with D being the PHE diffusion constants either in air (6.3×10^{-2} cm^2 s^{-1}) or water (7.5×10^{-6} cm^2 s^{-1}) and τ_{uz} and φ the tortuosity and porosity (0.4) of the medium.

Agar Test Track for Spatiotemporal Quantification of PHE Transport. A PDA patch (PosE; Ø: 1.4 cm, h.: 0.4 cm) inoculated with *P. ultimum* was placed in the center of a sterile polystyrene Petri dish. Two lateral agarose rectangles ($l \times w \times h$: 1.5 × 1 × 0.4 cm) containing 10 mM phosphate buffer were placed leaving a 0.1 cm air-filled gap between the agarose and PosE (Figure 1). Next to the outer end of each agarose rectangle, a PDA patch (Ø: 1.4 cm, h: 0.4 cm) was placed to promote growth of mycelia over the substrate-free agarose rectangles. Closed Petri dishes were incubated at room temperature (r.t.) in the dark. After mycelia had fully overgrown the system (ca. 5 d), 20 mg of solid PHE was added at PosH and cultivation continued. One, 2, 4, 24, and 48 h after the addition of PHE, triplicate test tracks were sacrificed and PHE contents of the central and the lateral patches analyzed. Prior to analysis the agarose rectangles were divided in three equally sized pieces (Figure 1). Except for PosH (point of PHE addition) PHE contents of PosB - PosG were individually quantified by gas chromatography-mass spectrometry (GC-MS) after extraction with 10 mL of acetone/hexane (1:3, v/v) for 24 h. Mycelia-free test tracks served as abiotic controls.

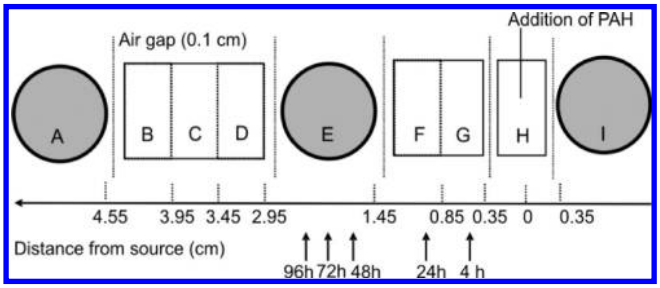

Figure 1. Schematic diagram of the agar test track for PAH transport. *P. ultimum* was inoculated on PosE which is flanked by lateral agar rectangles separated from the PDA patches (in gray) by a 0.1 cm air gap. Locations are indicated with capital letters (A to I for PosA to PosI). The air gap between PosG and PosH was omitted in the agar test track for spatiotemporal quantification of PHE transport to allow for PHE diffusion in agar patches PosF - PosH.

Agar Test Track for the Spatiotemporal Quantification of Transport of PAH Mixtures. Translocation of 16 two to six-ring PAH was quantified in the agar test track (Figure 1). The PosH patch was placed in a way leaving a 0.1 cm air-gap to neighboring PosG and PosI. Five μL of HMN containing 0.25 μg of each of the individual PAH (Table S1) were placed on PosH and PAH translocation measured on all positions after 24, 48, 72, and 96 h. Quantification of PAH was performed as for PHE. Mycelia-free test tracks served as abiotic controls.

Extraction and Instrumental Analysis. XAD4-entrapped PHE was extracted with an accelerated solvent extractor (ASE 200, Dionex; Germany) using PHE-d_{10} recovery standard. Samples were extracted five times with 3:1 (v/v) acetone/hexane; the extracts were concentrated and analyzed by GC (HP 6890 Series GC (Agilent, USA)) with a 30-m HP5MS

dx.doi.org/10.1021/es300810b | Environ. Sci. Technol. 2012, 46, 5463−5470

capillary column (Agilent, USA) and an Agilent 5973 MSD operating in selected ion monitoring mode (SIM). Detailed operating conditions have been previously described.[14]

Two-Photon Excitation Microscopy. A circular PDA patch (Ø = 1.5 cm, h: 0.1 cm) overgrown with *P. ultimum* was placed on a microscope slide at 1 cm distance to another PDA patch and the slide kept in the dark at r.t. until the mycelia bridged the PDA patches. Thereafter 10 μL of a saturated aqueous PHE solution was added, and the samples were covered with a glass coverslip. Two controls were prepared to assess the stability of the autofluorescence signals of PHE and the mycelia on PDA patches. Samples were analyzed with a Bio-Rad Radiance 2000 MP scanning system with a Spectra Physics Tsunami millennia laser (690−1050 nm) and mounted on an inverted microscope (Nikon Eclipse TE300) using a Nikon 20/0.75 Plan Fluor DIC water immersion lens. Autofluorescence of the mycelia and PHE were imaged simultaneously by excitation at 690 nm and fluorescence detection at 390 ± 35 nm (HQ 390/70) for *P. ultimum* and 495 ± 10 nm (HQ 495/20) for PHE, respectively. Images were taken and processed using Bio-Rad Lasersharp imaging software, Confocal assistant 4.02, and Amira 4.0 Software. The time lapsing images of PHE transport (512 × 512 pixel resolution) in the hyphal cytoplasm were scanned in a single optical plane at 1 s intervals for 1 to 1.9 min and used to quantify the velocity of cytoplasmic PHE translocation. 3D images of hyphae and spores were used to examine their total volumes and the volume of PHE-fluorescent vesicles. Transport of PHE along single hyphae ($M_{PHE;}$ nmol h^{-1}) was estimated by multiplying the average velocity v (μm h^{-1}) of vesicle translocation along hyphae, the volume fraction of vesicles exhibiting PHE autofluorescence (f_{vol}), the cross sectional area of a hypha (A; μm^2), and the concentration of PHE in lipid vesicles (C_v; nmol μm^{-3}) (eq 2)

$$M_{PHE} = v \times f_{vol} \times A \times C_v \quad (2)$$

C_v was estimated based on the membrane-buffer partitioning coefficient $\log_{MB} = 0.97 \log K_{OW} - 0.64$ with $\log K_{OW,PHE} = 4.46$[28] and a lipid density of 0.88 g L^{-1}.

RESULTS

Quantification of Mycelial PHE Transport. Phenanthrene translocation by mycelia was tested in a laboratory system mimicking water unsaturated porous habitats (Figure S1) using non-PHE degrading *P. ultimum* as model organism.[14] The time course of PHE accumulation in the XAD4 sink upon transport by *P. ultimum* is shown in Figure 2 by representing the difference of the net PHE mass transported in the presence and absence of mycelia (cf. Figure S2 for full data set). Visual inspection revealed that mycelia reached after 72 h the XAD4 resin which subsequently accumulated ≈820 nmol of PHE after t = 168 h. This results in an overall apparent PHE transport rate of ca. 4.9 nmol h^{-1} for the test system. Observed PHE transport rates were about 30- and 300-times higher than theoretical diffusive transport rates in either fully air-filled (0.13 nmol h^{-1}) or water-filled (0.014 nmol h^{-1}) pores (cf. eq 1) and about 2-fold higher than measured in mycelia-free controls (Figure S2), respectively. Such discrepancy between observed and theoretical abiotic PHE fluxes is unexpected and may point at an additional advective airborne PHE-transport in the test track. No matter what the reason of such difference, all these data indicate substantial active PHE mobilization by the mycelia of *P. ultimum*. To quantify the spatiotemporal mycelial PHE transport, an agar-based test track was used (Figure 1). It revealed clearly improved, i.e. active PHE transport by living mycelia. Figure 3 depicts the time course of PHE accumulation in PosB - PosE (i.e., locations separated from the PHE source by >1.45 cm including a 0.1-cm air gap) in the presence and absence of mycelia of *P. ultimum*. Effective PHE transport by *P. ultimum* over an air-filled space was quickly observed 4 h after addition of PHE (Figures 3 and 4). Abiotic (presumably vapor-phase) PHE transport was about 100-times lower than in the presence of *P. ultimum* (0.37 nmol vs 35 nmol, respectively). As compared to the column test tracks, the total amount of PHE

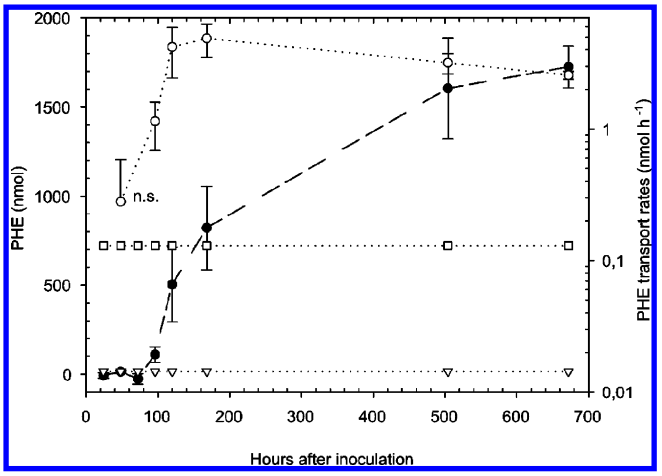

Figure 2. Time course of PHE extracted from XAD4 resins (filled circles) and PHE transport rates (open circles) in column test tracks (Figure S1). Data are the means and standard errors of $n \geq 3$ replicates and represent the difference of the PHE in the presence and absence of *P. ultimum* in order to solely depict mycelia-mediated PHE. The open triangles and squares represent the apparent diffusive PHE transport rates in water (triangles) and air (squares) assuming fully air- or water-filled pores. Open symbols refer to the logarithmic right y-axis (*n.s.* means that this data point is not statistically significant).

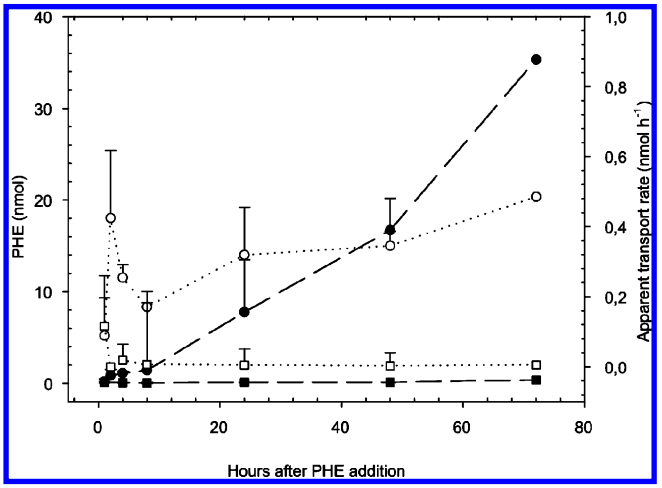

Figure 3. Time course of PHE extracted from locations PosB - PosE of the agar test track (Figure 1). Data are the means and standard errors of $n \geq 3$ replicates. Filled symbols represent the PHE accumulating after addition of 20 mg of solid PHE to PosH in the presence (circles) and absence of mycelia of *P. ultimum* (squares). Open symbols represent the corresponding apparent PHE transport rates in the presence (circles) and absence (squares) of mycelia of *P. ultimum* (right y-axis).

dx.doi.org/10.1021/es300810b | Environ. Sci. Technol. 2012, 46, 5463−5470

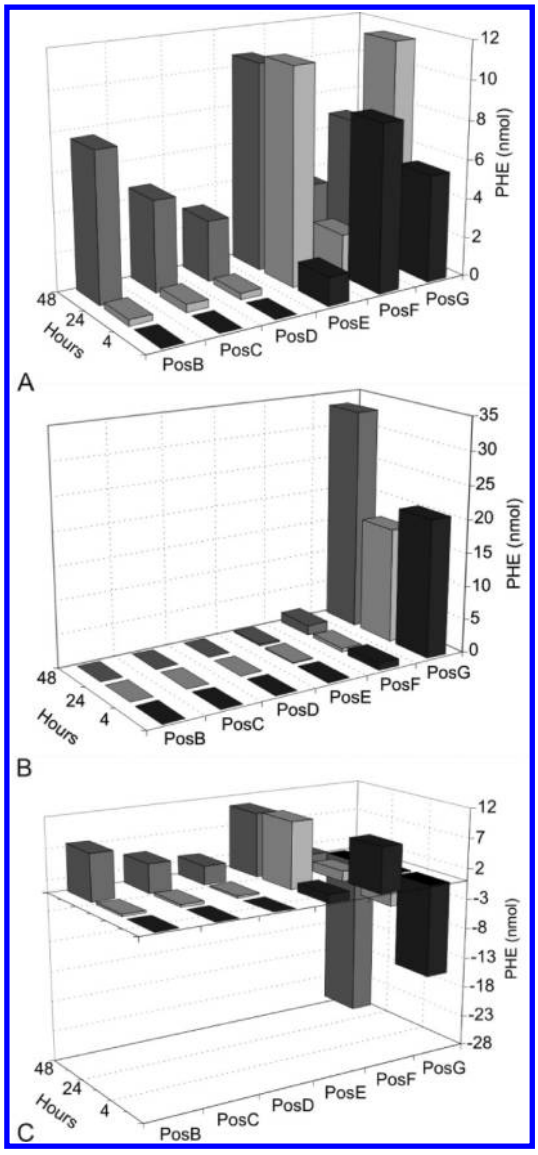

Figure 4. Spatiotemporal distribution of PHE on agar test tracks in the presence (part A) and absence of mycelia of *P. ultimum* (part B). Part C depicts the difference between data in parts A and B. Positive and negative values (at PosG near the source) indicate increased net mycelia-mediated PHE transport as compared to abiotic transport only. Data represent means of triplicate measurements.

transported by the mycelium was 10 to 15 times smaller (Figures 2 and 3). This may be explained by (i) the lower hyphal biomass on the agar relative to the column test track, (ii) the lack of the XAD4 sink for PHE driving the desorption of translocated PHE from the mycelia, and (iii) a possible increased PHE translocation by growing (column experiment) relative to pre-established mycelia (agar experiment). Spatiotemporal PHE quantification (Figure 4A,B) further revealed effective PHE transport to PosG - PosF (i.e., locations not separated from the PHE source by air gaps) and suggests elevated PHE transport in the presence of mycelia relative to aqueous diffusion in the controls (negative values in Figure 4C). Our data also show that *P. ultimum* increases total amounts of PHE translocated and hence improves its spatiotemporal distribution in the microcosm studied; positive and negative values (near the source) both indicate increased net mycelia-mediated PHE transport and underpin the active role of mycelial networks for PHE transport and dispersion (Figure 4C).

TPEM Visualization of PHE Translocation in Living P. ultimum. Two photon excitation microscopy (TPEM) was used to noninvasively visualize the movement of PHE (Figure 5A). Thirty minutes after addition, high PHE autofluorescence was observed associated with cytoplasmic vesicles of *P. ultimum* located near the source (Figure 5B). After 24 h, PHE autofluorescence was observed along most of the mycelium (Figure S3), with the highest densities in the subapical region where PHE-fluorescing vesicles occupied most of the volume of the cytoplasm. By analyzing 3-D images of the hyphae of *P. ultimum*, we were further able to quantify the volumes of spherical vesicles exhibiting PHE fluorescence (Figure 5C). On average 49% (15−81%; n = 15 visualization frames) of the cytoplasm volume was occupied by spherical vesicles exhibiting PHE autofluorescence. Remarkably distinct PHE autofluorescence was also detected in spores, with 0.2−80% of the spore's volume exhibiting PHE autofluorescence (Figure 5D). This accumulation of PHE in spores suggests the possibility of spore-mediated transport of PHE in the environment. Time lapse video micrographs of *P. ultimum* further demonstrated PHE translocation by cytoplasmic streaming at an average velocity of 13 ± 9 μm min^{-1} (n = 4) and a range of 4−21 μm min^{-1}.

Effect of PAH Structure on Active Hyphal Transport. We assessed whether mycelia also translocate other PAHs, particularly when present as oily mixtures typically occurring in contaminated sites. We applied artificial HMN-based oil containing 16 two to six-ring PAH to the mycelia of *P. ultimum* using the agar test track (Figure 1). The PAHs covered a log K_{OW} range of 3.3−6.8 (Table S1). In the presence of the mycelia and contrary to the abiotic control, only 3−30% of the initial mass of the individual PAH was recovered at the source (PosH) after 24 h (Figure S4). The significant losses of the low molecular weight PAH were likely due to their high vapor pressures (Table S1). In the presence of mycelia, all two and three-ring PAHs were spread over a wider area than could be explained by chemical diffusion (Figure S4). High levels of PAHs were detected on PosA and PosI likely due to effective PAH absorption in the elevated mycelial biomass formed in these positions in response to the presence of potato dextrose agar (PDA; Figure 1). Figure 6 depicts the apparent normalized transport rates to PosA and PosI. PAH transport rates to PosA (located beyond the diffusive distance of PAHs) depended on the PAH structure, i.e. extended over 5 orders of magnitude (Figure 6A) and seem to be inversely correlated to the log K_{OW} (Figure 6A). It is noteworthy that high molecular weight-PAHs were detected on PosA as late as 48 to 96 h after addition highlighting the low transport of these PAHs. Interestingly, observed transport rates to PosI (Figure 6B) were both significantly higher and less variable (≈0.03−0.07 nmol h^{-1}) likely due to an effective overlay of vesicle-driven and diffusive transport along the mycelia.

DISCUSSION

Visualization and Quantification of Hyphal PHE-Transport. Previous studies showed that bacteria move chemotactically along mycelia of *P. ultimum* which were brought in contact with a point source of a chemoattractant. Surprisingly, this was also observed, when air-filled spaces, which were only bridged by the fungal mycelium, separated the sources of nonvolatile attractants from the bacteria.[10] The

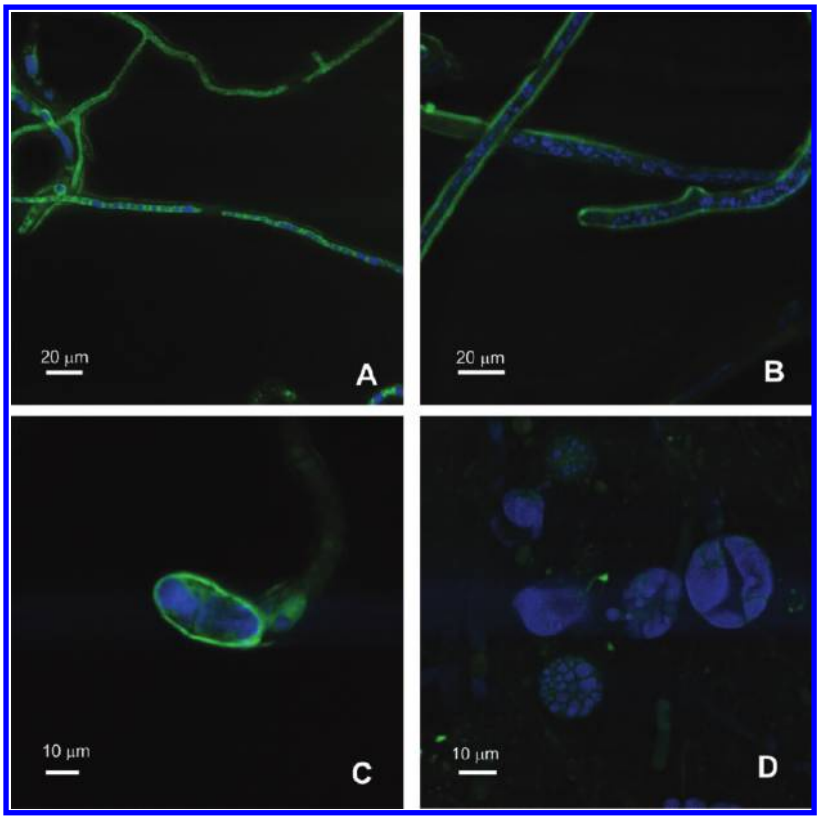

Figure 5. Two-photon excitation micrographs visualizing the accumulation of PHE (in blue) inside the hyphae of *P. ultimum* (in green) after 24 h (parts A-C) and in spores after 168 h of PHE addition (part D). Parts A and B: PHE is located in the spherical vesicles inside the hyphae at the growing tips. Part C: Close-up cross section through a hypha visualizing the accumulation of PHE in spherical vesicles. Part D: Accumulation of PHE inside spores.

translocation of chemicals along mycelia is an explanation for the build-up of the chemical gradient required for chemotaxis. In the present study, we observed that PHE was actively transported inside the mycelia of non-PHE degrading *P. ultimum*.[14] This led to an effective dispersion of this chemical in saturated and unsaturated habitats. Using TPEM, we also visualized active cytoplasmic translocation of PHE within living *P. ultimum* in a noninvasive way (Figure 6A). TPEM had been applied previously to demonstrate the uptake of PHE in living plants[29] or to estimate the rate of cytoplasmic lipid translocation within fungi.[25] Data from our transport experiments in columns and on agar test tracks (as well as TPEM visualization) revealed that the distribution of PHE in the presence of mycelia is more effective and extends over longer distances than diffusive transport in air and/or water. This underpins earlier data[27] showing metabolically driven substrate-carbon translocation away from a glucose-containing domain by actively growing *Rhizoctonia solanii* in nutrionally heterogeneous microcosms. We estimated 10−100-fold enhanced transport rates relative to diffusion, observed PHE at locations not reached in the absence of mycelia (e.g., due to the lack of continuous aqueous diffusion paths), and directly visualized the movement of PHE-containing vesicles by cytoplasmic streaming. From successful staining experiments using the lipophilic probe FM4-64 (Invitrogen) to stain plasma membranes of *P. ultimum* (data not shown), our TPEM microscopic observations and previous observations that PHE partitions into hyphal vesicle lipids,[22] we can conclude that long-range PHE transport is primarily due to the streaming of cytoplasmic vesicles after uptake and absorption by their lipid contents; whereas, diffusion into the cytoplasm and along aqueous films forming outside the hyphae seem to play minor roles at best. Using a cross sectional area of the pore space $A_{ec} = 3.1 \times 10^7\ \mu m^2$ and assuming that either 1% (minimum estimate) or 50% of A_{ec} (maximum estimate) are occupied by hyphae of $5.9 \pm 1.2\ \mu m$ diameter ($n = 15$), it was calculated that 4500 (1%) or 227,000 hyphae (50%) are available to transport PHE in the column test track. Thus, experimental PHE transport rates of 4.9 nmol h^{-1} would result in ≈0.02 to 1.1 pmol (≈4 to 200 pg) transported per hypha per hour over a distance of 1 cm. The significance for the ecology of contaminant biodegradation might be illustrated by the fact that these masses correspond to either 12 or 600 times the dry weight of a typical bacterium (≈0.3 pg). Interestingly, similar average PHE transport rates through a hyphal cross section of *P. ultimum* were estimated (M = 1.0 pmol h^{-1}) from independent TPEM observations (eq 2). The effective PHE accumulation in XAD4 in column experiments also suggests that translocated PHE may indeed effectively partition into the PHE-free neighborhood of mycelia. From a bioremediation perspective this indicates that mycelial PHE may be continuously available to bacteria in remote sink regions and, hence, promote faster cleanup of PAH contaminated soil.

Translocation of PAH-Mixtures. Figure 6 shows that mycelia of *P. ultimum* facilitated the distribution of a wide range of PAH in both water- and air-filled environments. Apparent transport rates were dependent on PAH-structure, the mycelial biomass, and the position of the sink region studied relative to the PAH source (Figure 6). Elevated and poorly variable transport rates were observed at positions within diffusion distance of PAH (PosI); whereas, PAH transport rates to the

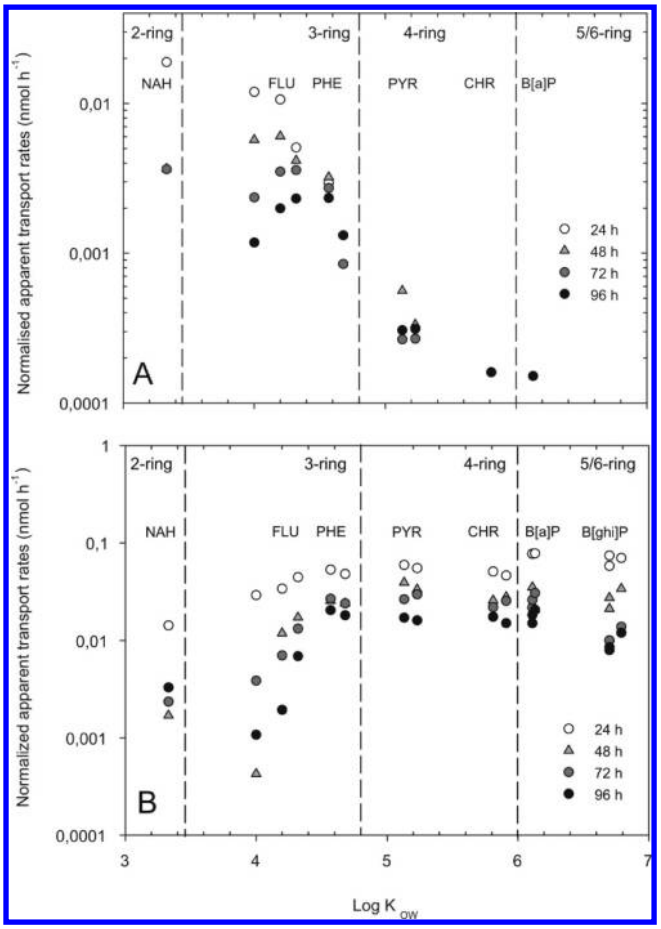

Figure 6. Transport rates of 16 PAH of varying KOW (Table S1) to PosA (part A) and PosI (part B) situated at 5 and 1 cm from the PAH source (PosH), in the agar test track (Figure 1). Data are means of triplicates and are calculated from the differences of normalized molar PAH amounts in the presence and absence of the mycelia of *P. ultimum* in order to solely quantify mycelia-mediated PHE transport. As equal weight concentrations (0.25 μg per 5 μL) instead of equal molarities of the individual PAH were added, transport rates of PAH were normalized to the mol amount of NAH (1.95 nmol) for better comparison.

more distant PosA varied by several orders of magnitude. The reason for these observations is unknown; however, two distinct mechanisms of nutrient translocation (and variations thereof) have been described in the literature: passive translocation (i.e., diffusion) and active, metabolically driven transport.[30] Variations may include (i) passive translocation combined with active uptake and translocation, (ii) active, cytoplasmic translocation and pressure-driven bulk flow, (iii) physical translocation by external movement of a substance by capillary action and diffusion along hyphal walls (cf. ref 31). Higher rates of the non-nutrient PHE to PosI are likely to be explained by an overlay of vesicle-driven and diffusive transport along mycelia; whereas, transport of the two to four-ring PAHs and B[a]P to PosA is likely due to cytoplasmic streaming of lipid vesicle-bound PAHs alone. Corresponding transport rates were correlated with the chemical log K_{OW} of the PAHs (Figure 6A), with B[a]P exhibiting a ca. 2 orders of magnitude lower transport rate than NAH. As the velocity of the cytoplasmic vesicles is independent of individual PAH structures, the observed rate differences may depend on varying PAH-uptake rates which, in turn, are a function of PAH aqueous solubility. In order to enter the mycelial cytoplasm and to be transported by vesicles PAHs need to (i) reach the cell surface (i.e., be bioavailable), (ii) pass through the cell wall into the cytoplasm,[32] and (iii) diffuse within the cytoplasm before association with vesicles. Although diffusion through the plasma membrane has been proposed to be the rate limiting and discriminating step of cellular uptake of hydrocarbons of varying hydrophobicity, Verdin et al.[22] more recently observed that uptake and storage of PAHs in fungi was independent of chemical structure. Regardless of the exact mechanism by which PAHs are taken up, TPEM data have indicated that PAHs accumulate in lipid vesicles that are likely to consist of a hydrophobic core of neutral storage lipids enclosed by a phospholipid monolayer with embedded proteins.[33] Fungi, oomycetes, and yeasts are widely known to store their excess carbon as TAG, which can comprise over 90% of the lipids and are also found in large amount in developing spores.[25,34] This observation correlates well with our TPEM observation of PHE accumulation in lipid vesicles and spores in *P. ultimum* (Figure 5D).

Relevance for PAH Biodegradation. The coexistence of bacteria and fungi in soil and their known catabolic cooperation suggest that physical interactions between them may be important for PAH degradation.[2,6] PAH biotransformation in soil is often limited by their low availability to degrading microorganisms. This limitation is caused by restricted mobility of soil bacteria and retarded transfer of organic contaminants.[3] Besides some bioturbation, mixing hardly occurs in soil, and the effective diffusion of molecules may be orders of magnitude lower than in water, since the diffusion is retarded by the solid phases, dead-end pores, and the high tortuosity of the pore system. Bacterial cells are often excluded from pores <0.2−0.8 μm, and they are incapable of passing through air−water interfaces. Consequently, a large fraction of PAH-degrading bacteria in soil is expected to be physically separated from PAH-sources and dependent on diffusive transport of PAHs from the PAH-sources to the cells.[35] Former work has shown that mycelia facilitate both the random and chemotactic movement of contaminant degrading bacteria ('fungal highways')[9,10,14] and thereby improve the accessibility of bacteria to soil contaminants for improved biodegradation.[36] In this work we present evidence that mycelia additionally are able to increase the mobility of PAHs by actively translocating them by their cytoplasmic streaming ('hyphal pipelines').

Cytoplasmic transport of lipid vesicles is universal both to septated and nonseptated hyphal organism. Vesicle-bound PAH transport hence may also be expected by hyphae of other, physiologically, functionally, and phylogenetically very different mycelial organisms. Likewise, it can be assumed that PAH-degrading fungi may transport PAHs by cytoplasmic streaming to the hyphal tips where, upon release, they may become available both to bacteria and fungal PAH-degrading enzymes.[2] Free-living and mycorrhizal fungi are also involved in other functions in soil remediation schemes. They metabolically or cometabolically transform a wide range of organic contaminants,[37] transfer plant-derived organic substrates to nonsymbiotic soil microorganisms, penetrate soil aggregates, or promote the transport of water in dry environments.[38] It is hence not daring to speculate that mycelia may also actively transport a wide range of readily water-soluble (anthropogenic) compounds and hence increase their bioaccessibility in air-filled environmental systems. Fungal mycelia are also known to produce large quantities of exudates that can serve as auxiliary

carbon sources for pollutant-degrading bacteria and thereby stimulate their activity and diversity.[39] The use of plants for the alimentation of mycorrhizal or other autochthonous fungi themselves may further be a promising avenue for enhanced rhizosphere bioremediation of organic contaminants. The low degree of mechanical intervention in plant-based natural attenuation of soil is highly likely to favor the establishment of filamentous fungi. Due to their ubiquity and length, we therefore assume that mycelial networks play a significant role in increasing the physical processes between indigenous microbes and contaminants for the microbial ecosystem service of contaminant biodegradation in soil and, hence, provide a poorly appreciated, untapped potential for biotechnological remediation approaches. Given the actual demand of sustainable, cheap, and tailor-made technologies, there is considerable thrust to translate powerful ecosystem services, such as those provided by mycelia, into ecology-based bioremediation technologies.[2]

■ ASSOCIATED CONTENT

Supporting Information

One table and four figures. This material is available free of charge via the Internet at http://pubs.acs.org.

■ AUTHOR INFORMATION

Corresponding Author

*Phone: +49 341 235 1316. Fax: +49 341 235 1316. E-mail: lukas.wick@ufz.de.

Notes

The authors declare no competing financial interest.

■ ACKNOWLEDGMENTS

Funding by the European grant MC-EST 20984 (RAISEBIO) and the Helmholtz Association via the program topic "CITE - Chemicals in the Environment" is acknowledged. The authors thank J. Dent for technical help with the TPEM study and Megan Gignac, Birgit Würz, Rita Remer, and Jana Reichenbach for skilled experimental help.

■ REFERENCES

(1) Bosma, T. N. P.; Middeldorp, P. J. M.; Schraa, G.; Zehnder, A. J. B. Mass transfer limitation of biotransformation: Quantifying bioavailability. *Environ. Sci. Technol.* **1997**, *31* (1), 248−252.

(2) Harms, H.; Schlosser, D.; Wick, L. Y. Untapped potential: exploiting fungi in bioremediation of hazardous chemicals. *Nat. Rev. Microbiol.* **2011**, *9* (3), 177−192.

(3) Johnsen, A. R.; Wick, L. Y.; Harms, H. Principles of microbial PAH degradation. *Environ. Pollut.* **2005**, *133*, 71−84.

(4) Ritz, K.; Young, I. M. Interactions between soil structure and fungi. *Mycologist* **2004**, *18*, 52−59.

(5) Ferguson, B. A.; Dreisbach, T. A.; Parks, C. G.; Filip, G. M.; Schmitt, C. L. Coarse-scale population structure of pathogenic *Armillaria* species in a mixed-conifer forest in the Blue Mountains of northeast Oregon. *Can. J. Forest Res.* **2003**, *33* (4), 612−623.

(6) Frey-Klett, P.; Burlinson, P.; Deveau, A.; Barret, M.; Tarkka, T.; Sarniguet, A. Bacterial-Fungal Interactions: Hyphens between Agricultural, Clinical, Environmental, and Food Microbiologists. *Microbiol. Mol. Biol. Rev.* **2011**, *75* (4), 583−609.

(7) Johansson, J. F.; Paul, L. R.; Finlay, R. D. Microbial interactions in the mycorrhizosphere and their significance for sustainable agriculture. *FEMS Microbiol. Ecol.* **2004**, *48* (1), 1−13.

(8) Wessels, J. G. H. Hydrophobines, proteins that change the nature of the fungal surface. *Adv. Microbiol. Physiol.* **1997**, *38*, 1−45.

(9) Kohlmeier, S.; Smits, T. H. M.; Ford, R.; Keel, C.; Harms, H.; Wick, L. Y. Taking the fungal highway: Mobilization of pollutant degrading bacteria by fungi. *Environ. Sci. Technol.* **2005**, *39*, 4640−4646.

(10) Furuno, S.; Päzolt, K.; Rabe, C.; Neu, T.; Harms, H.; Wick, L. Fungal mycelia allow chemotactic dispersla of PAH-degrading bacteria in water-unsaturated systems. *Environ. Microbiol.* **2010**, *12* (6), 1391−1398.

(11) Nazir, R.; Warmink, J. A.; Boersma, H.; van Elsas, J. D. Mechanisms that promote bacterial fitness in fungal-affected soil microhabitats. *FEMS Microbiol. Ecol.* **2010**, *71* (2), 169−185.

(12) Banitz, T.; Fetzer, I.; Johst, K.; Wick, L. Y.; Frank, K. Assessing biodegradation benefits from dispersal networks. *Ecol. Model.* **2010**, *222*, 2552−2560.

(13) Banitz, T.; Wick, L. Y.; Fetzer, I.; Frank, K.; Harms, H.; Johst, K. Dispersal networks for enhancing bacterial degradation in heterogeneous environments. *Environ. Pollut.* **2011**, *159* (10), 2781−2788.

(14) Wick, L. Y.; Remer, R.; Würz, B.; Reichenbach, J.; Braun, S.; Schäfer, F.; Harms, H. Effect of Fungal Hyphae on the Access of Bacteria to Phenanthrene in Soil. *Environ. Sci. Technol.* **2007**, *41*, 500−505.

(15) Darrah, P. R.; Tlalka, M.; Ashford, A.; Watkinson, S. C.; Fricker, M. D. The Vacuole System is a Significant Intracellular Pathway for Longitudinal Solute Transport in Basidiomycete Fungi. *Eukariot. Cell* **2006**, *5* (7), 1111−1125.

(16) Bebber, D. P.; Hynes, J.; Darrah, P. R.; Boddy, L.; Fricker, M. D. Biological solutions to transport network design. *Proc. R. Soc.* **2007**, *274* (1623), 2307−2315.

(17) Suelmann, R.; Sievers, N.; Fischer, R. Nuclear traffic in fungal hyphae: in vivo study of nuclear migration and positioning in *Aspergillus nidulans*. *Mol. Microbiol.* **1997**, *25* (4), 757−769.

(18) Ross, I. K. Nuclear migration rates in *Coprinus congregatus* - new record. *Mycologia* **1976**, *68* (2), 418−422.

(19) Wick, L. Y.; Furuno, S.; Harms, H. Fungi as transport vectors for contaminants and contaminant-degrading bacteria. In *Handbook of Hydrocarbon Microbiology*; Timmis, K., Mc Genity, T., van der Meer, J. R., Eds.; Springer-Verlag: Berlin, Heidelberg, NY, 2010; pp 1555−1561.

(20) Tobin, J. M.; White, C.; Gadd, G. M. Metal accumulation by fungi: Applications in environmental biotechnology. *J. Ind. Microbiol.* **1994**, *13* (2), 126−130.

(21) Clark, R. B.; Zeto, S. K. Mineral acquisition by arbuscular mycorrhizal plants. *J. Plant Nutr.* **2000**, *23* (7), 867−902.

(22) Verdin, A.; Lounes-Hadj-Sahraoui, A.; Newsam, R.; Robinson, G.; Durand, R. Polycyclic aromatic hydrocarbons storage by *Fusarium solani* in intracellular lipid vesicles. *Environ. Pollut.* **2005**, *133*, 283−291.

(23) Kaeppeli, O.; Fiechter, A. Mode of Interaction Between Substrate and Cell-Surface of hydrocarbon-Utilizing Yeast *Candida Tropicalis*. *Biotechnol. Bioeng.* **1976**, *18* (7), 967−974.

(24) Sikkema, J.; de Bont, J. A. M.; Poolman, B. Mechanism of membrane toxicity of hydrocarbons. *Microbiol. Rev.* **1995**, *59* (2), 201−222.

(25) Bago, B.; Zipfel, W.; Williams, R. M.; Jun, J.; Arreola, R.; Lammers, P. J.; Pfeffer, P. E.; Shachar-Hill, Y. Translocation and Utilization of Fungal Storage Lipid in the Arbuscular Mycorrhizal Symbiosis. *Plant Physiol.* **2002**, *128*, 108−124.

(26) Maurhofer, M.; Keel, C.; Schnider, U.; Voisard, C.; Haas, D.; Défago, G. Influence of enhanced antibiotic production in *Pseudomonas fluorescens* strain CHA0 on its disease suppressive capacity. *Phytopathology* **1992**, *82*, 190−195.

(27) Schwarzenbach, R. P.; Gschwend, P. M.; Imboden, D. M. *Environmental Organic Chemistry*, 1st ed.; John Wiley & Sons, Inc.: Hoboken, NJ, 2003.

(28) Sikkema, J.; de Bont, J. A. M.; Poolman, B. Interactions of Cyclic Hydrocarbons with Biological-Membranes. *J. Biol. Chem.* **1994**, *269* (11), 8022−8028.

(29) Wild, E.; Dent, J.; Barber, J. L.; Thomas, G. O.; Jones, K. C. A novel analytical approach for visualizing and tracking organic chemicals in plants. *Environ. Sci. Technol.* **2004**, *38* (15), 4195−4199.
(30) Olsson, S. Mycelial density profiles of fungi on heterogeneous media and their interpretation in terms of nutrient reallocation patterns. *Mycol. Res.* **1995**, *99*, 143−153.
(31) Jacobs, H.; Boswell, G. P.; Scrimgeour, C. M.; Davidson, F. A.; Gadd, G. M.; Ritz, K. Translocation of carbon by *Rhizoctonia solani* in nutritionally-heterogeneous microcosms. *Mycol. Res.* **2004**, *108*, 453−462.
(32) Hamilton, J. A.; Johnson, R. A.; Corkey, B.; Kamp, F. Fatty acid transport - The diffusion mechanism in model and biological membranes. *J. Mol. Neurosci.* **2001**, *16* (2−3), 99−108.
(33) van Aarle, I. M.; Olsson, P. A. Fungal lipid accumulation and development of mycelial structures by two arbuscular mycorrhizal fungi. *Appl. Environ. Microbiol.* **2003**, *69* (11), 6762−6767.
(34) Allaway, W. G.; Ashford, A. E.; Heath, I. B.; Hardham, A. R. Vacuolar reticulum in oomycete hyphal tips: An additional component of the Ca^{2+} regulatory system? *Fungal Genet. Biol.* **1997**, *22* (3), 209−220.
(35) Harms, H.; Bosma, T. N. P. Mass transfer limitation of microbial growth and pollutant degradation. *J. Ind. Microbiol. Biotechnol.* **1997**, *18*, 97−105.
(36) Semple, K. T.; Doick, K. J.; Wick, L. Y.; Harms, H. Microbial interactions with organic contaminants in soil: Definitions, processes and measurement. *Environ. Pollut.* **2007**, *150* (1), 166−176.
(37) Pinedo-Rivilla, C.; Aleu, J.; Collado, I. G. Pollutants Biodegradation by Fungi. *Curr. Org. Chem.* **2009**, *13* (12), 1194−1214.
(38) Allen, M. F. Mycorrhizal fungi: Highways for water and nutrients in arid soils. *Vadose Zone J.* **2007**, *6* (2), 291−297.
(39) Federici, E.; Leonardi, V.; Giubilei, M. A.; Quaratino, D.; Spaccapelo, R.; d'Annibale, A.; Petruccioli, M. Addition of allochthonous fungi to a historically contaminated soil affects both remediation efficiency and bacterial diversity. *Appl. Microbiol. Biotechnol.* **2007**, *77* (1), 203−211.